

A Liquid-Crystalline Silsesquioxane Dendrimer Exhibiting Chiral Nematic and Columnar Mesophases

Isabel M. Saez,*^[a] John W. Goodby,*^[a] and Robert M. Richardson^[b]

Abstract: A hexadecamer, first-generation, octasilsesquioxane liquid-crystalline dendrimer was synthesized by a platinum-catalyzed hydrosilylation reaction of the parent first-generation vinyl octasilsesquioxane dendrimer with a modified, laterally substituted mesogen. The structure and purity of the octasilsesquioxane substrate was confirmed by ¹H, ¹³C, and ²⁹Si NMR spectroscopy,

microanalysis, and size exclusion chromatography (SEC). The mesogenic substrate was found to exhibit only a chiral nematic phase, whereas the resulting hexadecamer dendrimer displays enan-

tropic chiral nematic, disordered hexagonal columnar, and disordered rectangular columnar phases, with a glass transition below room temperature. The lateral or side-on attachment of the mesogen to the dendritic core was found to be a key design feature in the formation of the mesophases.

Keywords: chiral nematic phases • columnar phases • dendrimers • liquid crystals • silsesquioxane

Introduction

Over recent years, extensive research into hyperbranched and dendritic polymer systems has created a new and distinct field of materials research.^[1] The developing subject of hyperbranched systems has also strongly influenced the field of liquid crystals, with the result that there is now a growing number of dendritic liquid-crystal polymers (LCPs) reported in the literature. Dendritic, as well as hyperbranched, liquid-crystal polymers in which the mesogenic groups form part of each branching unit have been reported by the groups of Percec^[2] and Ringsdorf.^[3] Dendrimers without mesogenic groups, reported by Lattermann,^[4] Percec,^[5] Moore,^[6] Meier,^[7] and Frey,^[8b] have been shown to be liquid crystalline; however, the origin of the mesophase formation in these cases is different to dendrimers that possess conventional mesogenic units. A different approach has been used in the synthesis of liquid-crystal, functionalized dendrimers; they

differ from the above dendritic LCPs in that the mesogenic groups are located on the surface of the dendritic scaffold, usually by modification of the pre-formed scaffold by mesogenic end groups. Dendrimers based on carbosilane and carbosiloxane,^[8–10] ferrocene and ferrocene–fullerene,^[11] aliphatic polyester,^[12] polyamidoamine,^[13] and poly(propylene imine)^[14] have been reported; however, in almost all cases the formation of smectic (Sm) phases was observed.

Recently we reported a dendritic LCP based on the cubic silsesquioxane core, with sixteen cyanobiphenyl mesogenic groups attached to its corners, that exhibits SmA and SmC mesophases.^[15] Octasilsesquioxane thus provides a very useful central core for the synthesis of dendritic LCPs because it has eight primary (radial) branches for derivatization, allowing the dense-packing limit to be reached at early generations. Moreover, the rigid framework of the octasilsesquioxane core offers the possibility of a contrasting comparison with dendrimers derived from entirely flexible scaffolds as described above.^[8–10, 13, 14]

A limited number of examples of monomeric LC polyhedral silsesquioxane materials have been reported.^[16] Two approaches have been followed to produce nematic (N) silsesquioxanes; i) the first silsesquioxane nematogen reported was created through the lateral attachment of mesogens to the silsesquioxane core,^[16a] recently a new example following this approach has been described;^[16i] and ii) a completely different approach that utilizes partial substitution of the cubic core.^[16f]

Our approach to chiral LC dendrimers is based on the functionalization of the parent hexadecavinyl dendrimer **2** (see Scheme 1 below),^[15, 17] with chiral mesogens. We targeted specifically the induction of a N* phase, owing to its extensive

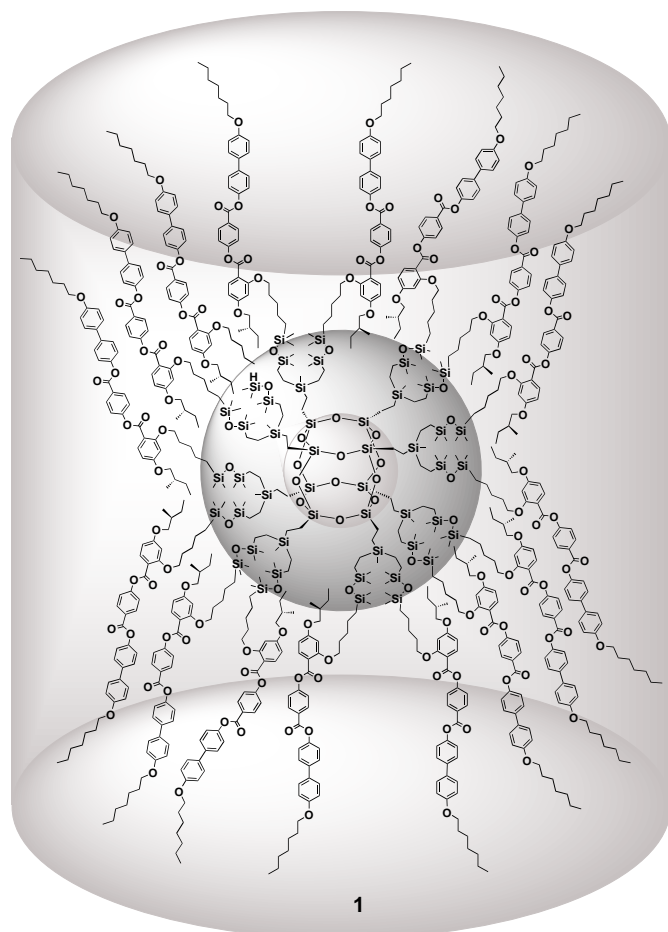
[a] Prof. J. W. Goodby, Dr. I. M. Saez
Department of Chemistry, University of Hull
Hull HU6 7RX (UK)
Fax: (+44) 1482-466411
E-mail: j.w.goodby@chem.hull.ac.uk
i.m.saez@chem.hull.ac.uk

[b] Prof. R. M. Richardson
HH Wills Physics Laboratory, University of Bristol
Bristol BS8 1TL (UK)
Fax: (+44) 1179-255624

Supporting information for this article is available on the WWW under <http://www.wiley-vch.de/home/chemistry/> or from the author. SEC trace of dendrimer **1** (THF solution; flow marker: toluene). ²⁹Si NMR spectrum of **1** (CD₂Cl₂).

applications in light-driven optical devices,^[18] by the lateral or side-on attachment of mesogens to the dendritic scaffold, as previously demonstrated for related laterally substituted side-chain LC polymers.^[19] In addition, the introduction of chirality into spherical dendritic systems provides an opportunity to examine the potential for materials to have molecular defects based on the chirality of the system in a similar way to how, on the mesoscopic scale, boojums are found in chiral nematic phases.

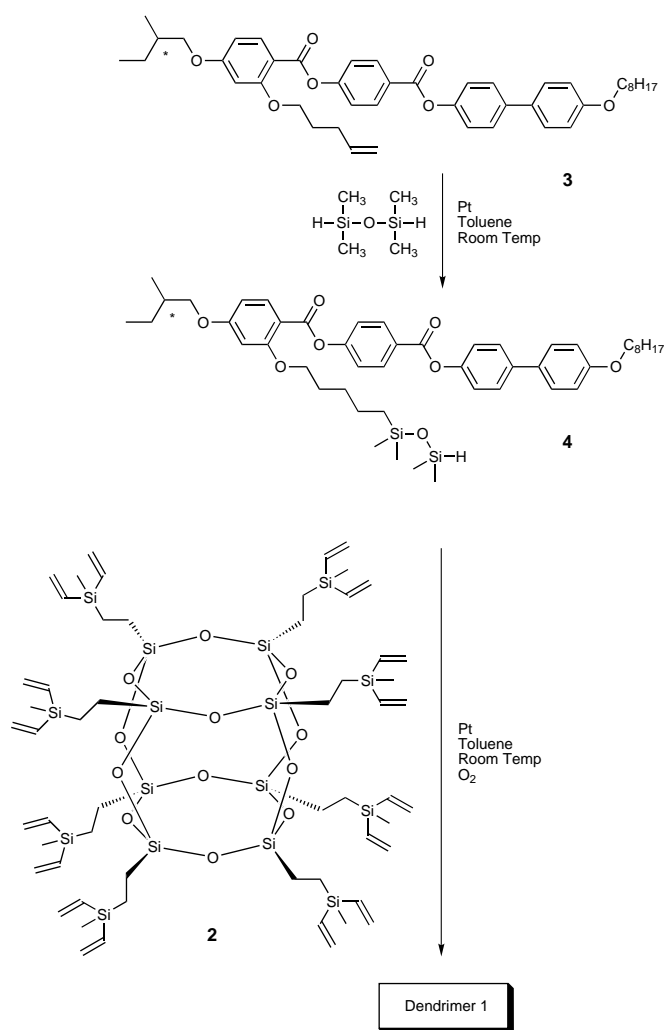
Thus, in this article we present the design, synthesis, characterization, and phase behavior of the first-generation dendrimer **1**, based on the silsesquioxane core, which has



sixteen side-on attached mesogenic units and exhibits chiral nematic (N^*), hexagonal disordered columnar (Col_{hd}), and rectangular disordered columnar (Col_{rd}) phases.

Results and Discussion

The synthesis of dendritic LCP **1** is presented in Scheme 1. The alkene functionality of the mesogenic precursor (*S*)-4'-octyloxybiphenyl-4-yl 4-[4-(2-methylbutoxy)-2-(pent-4-enyloxy)benzoyloxy]benzoate (**3**)^[19c] was converted to a silane by platinum-catalyzed hydrosilylation of **3** with an excess of tetramethyl disiloxane at room temperature by using Karstedt's catalyst; this afforded the novel hydridosiloxane **4** in



Scheme 1.

58% yield. Substrate **4** was grafted onto **2** by a similar Pt-catalyzed hydrosilylation in toluene at room temperature with Karstedt's catalyst, with a 1.3:1 ratio of **4** per vinyl group to obtain complete reaction. Product **1** was purified by column chromatography over silica gel and isolated as a white glassy material in 35% yield.

Compound **4** showed the expected features in the ^1H NMR spectrum, notably a septet at $\delta = 4.64$, due to the Si–H resonance, and the exclusive formation of the α -isomer from the addition of the Si–H bond to the terminal alkene. ^{29}Si NMR spectroscopy confirmed the presence of two M-type silicon atoms in slightly different environments, at $\delta = 9.79$ (O–Si–CH₂) and $\delta = -6.73$ (O–Si–H).

Dendrimer **1** was characterized by multinuclear magnetic resonance. ^1H NMR spectroscopy showed well-resolved resonances for all the protons in the molecule, indicating rapid relaxation processes at room temperature pointing to a high degree of freedom of the internal structure of the molecule about the silsesquioxane cage. Complete disappearance of the vinylic protons of **2** indicate full conversion to **1**. As previously encountered,^[15] the two different Si–CH₂–CH₂–Si disilylethylene segments, belonging to generation zero and generation one, respectively, could not be

differentiated and appear as two overlapping pseudotriplets at $\delta = 0.49$ and 0.35 . Within the limit of detection, the addition of the Si–H bond to the silylvinyl group is regiospecific, affording only the β -addition product, as confirmed by the ^{13}C NMR spectrum. The two sets of Si(CH₃) protons appeared as two very close singlets, indicating a slight difference in chemical environment.

Most of the information gleaned about the nature and symmetry of **1** was obtained from the ^{29}Si NMR spectrum; the T silicon appears as a singlet at $\delta = -66.3$, an indication that the core remains intact during the hydrosilylation reaction and that it is symmetrically substituted. The resonance of the branching point silicon atom is shifted appropriately from a singlet at $\delta = -11.0$ in **2** to a singlet at $\delta = 7.23$ for **1** with respect to the change from vinylic to ethylene substitution. The silicon atoms of the tetramethyldisiloxane connector group appear as two close singlets at $\delta = 8.30$ and 7.93 .

Dendritic LCP **1** was found to be essentially monodisperse as shown by the single symmetrical peak of dispersity 1.01 found by SEC chromatography in THF [$M_w = 10912$, $M_n = 10750$, polydispersity $\gamma = 1.01$; M_w (calcd) = 14653]. However, the molecular weight is underestimated because of the “apparent” smaller hydrodynamic volume, which is most probably due to the globular shape of the molecule, in contrast to that of the coiled conformation of the polystyrene standards. This effect has also been observed in other types of mesogen-functionalized dendrimers.^[8b, 12, 14b, 15] Mass determination by MALDI spectrometry (2,5-dihydroxybenzoic acid matrix, KCl cationization agent) did not provide an exact mass; however, a broad peak with maximum centered around the expected value was observed. Moreover, a broad peak assigned to the doubly-charged molecular entity was also observed.

The mesomorphic properties of the mesogenic subunit (**4**) and the final dendritic product (**1**) were investigated by differential scanning calorimetry (DSC) and transmitted polarized light microscopy (POM). The mesogenic precursor **4** was shown to exhibit only an enantiotropic chiral nematic (N*) phase [K 73.6 ($\Delta H = 32.2 \text{ kJ mol}^{-1}$) N* 88.2 °C isotropic liquid ($\Delta H = 0.59 \text{ kJ mol}^{-1}$)].

The DSC thermogram of the dendritic LCP **1** is displayed in Figure 1 (scan rate $10^\circ \text{ min}^{-1}$). Upon heating a pristine sample, which is in a glassy state at room temperature, the material shows a very weak endotherm at 88.8°C and a broad peak with an onset at 100.0°C that overlaps with a sharper endotherm of onset 109.0°C , which is associated with the transition between the liquid-crystal state and the isotropic liquid. However, the resolution of the overlapping endotherms did not improve on reducing the heating rate to $2^\circ \text{C min}^{-1}$. The cooling cycle from the isotropic state proved much more informative as the transitions between the mesophases were better resolved. Firstly, the sample displays a sharp exotherm for the transition from the isotropic liquid to the N* phase at 107.7°C ($\Delta H = 0.66 \text{ kJ mol}^{-1}$ per mesogen). Cooling promoted a second transition between the N* and the Col_{hd} phases at 102.3°C ($\Delta H = 0.67 \text{ kJ mol}^{-1}$ per mesogen). A very weak and broad exotherm was observed between 87 and 81°C with an onset of 86.5°C ($\Delta H = 0.67 \text{ kJ mol}^{-1}$). The broadness of the enthalpy suggests that the change is more

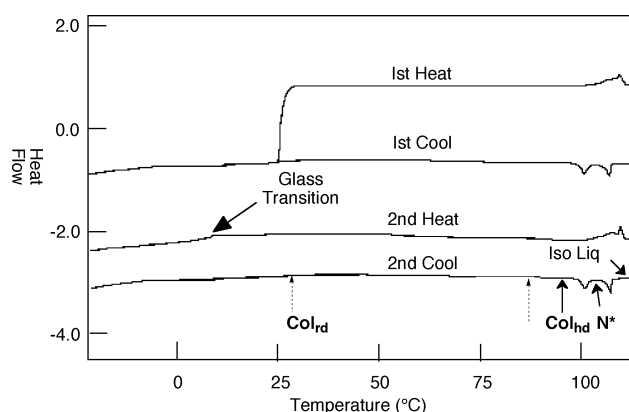


Figure 1. Differential scanning thermogram (heating and cooling rates taken at $10^\circ \text{ min}^{-1}$) of dendritic LCP **1**.

likely to be associated with a kinetic event rather than a phase transition. No further enthalpy changes were detected upon cooling other than a broad glass transition at approximately 5.4°C . Thus, the further transition to the proposed rectangular disordered columnar phase (observed by POM and X-ray diffraction) was not detected by calorimetry.

The optical textures of the compound were examined by polarized optical microscopy (POM). On cooling the isotropic liquid, the sample rapidly develops focal-conic domains at 107°C ; the domains evolve to give a Grandjean plane texture within a 2°C range (see Figure 2, top) from the isotropization point; the presence of this texture unequivocally identifies the phase as a chiral nematic (N*) phase. Further cooling to 102.3°C induces the formation of needles that coalesce to give the fanlike texture of a hexagonal columnar phase (Figure 2, middle). The absence of any elliptical and hyperbolic lines of optical discontinuity, coupled with the formation of optically extinct homeotropic areas confirms the classification of the phase as hexagonal columnar. Cooling this phase resulted in another change in texture with the fanlike domains of the hexagonal columnar phase becoming broken with grainy edges, whereas the homeotropic areas developed domains that display parallel dark and bright lines (Figure 2, bottom). The small sizes of the domains formed did not allow us to conclusively identify this phase; however, the observations suggest that it could be a rectangular columnar phase.

Powder X-ray diffraction studies confirmed the initial structural classifications for the mesophases observed by polarized optical microscopy. At high temperatures (~ 70 to 100°C) the columnar phase exhibits only one diffraction peak, but upon cooling to approximately 70°C a set of three peaks, in the ratio of 1:3:4, developed indicating the presence of a hexagonal phase. Table 1 gives the relative intensities of the first peaks and the inter-columnar distances (\AA) as a function of temperature ($^\circ \text{C}$). On cooling the columnar phase through the temperature range of 75 to 65°C , over which the number of observed diffraction peaks increases, no sudden change occurs in the position of the first peak, and, hence, the inter-columnar spacings (for a hexagonal lattice) remain much the same. This suggests that there is a strengthening of the ordering at $\sim 70^\circ \text{C}$, but no change in the symmetry of the phase. Thus at high temperatures the phase is probably

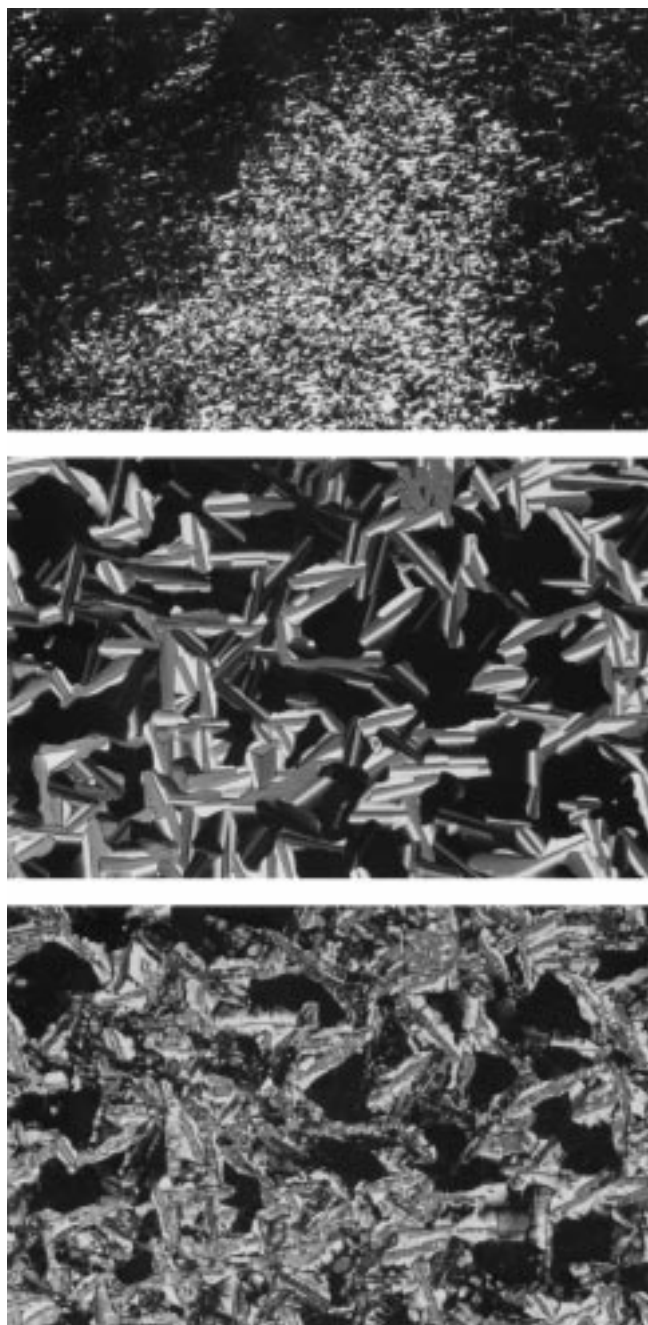


Figure 2. Top: The Grandjean texture of the chiral nematic phase ($\times 100$). Middle: The fan and homeotropic texture of the disordered hexagonal columnar phase ($\times 100$). Bottom: the broken fan and mosaic texture of biaxial disordered rectangular phase ($\times 100$).

disordered so that only the first (110) diffraction peak is observed; at lower temperatures the phase becomes better organized thereby allowing us to observe the 210 and 220 peaks.

Upon further cooling to approximately 30°C , the lowest peak of the diffraction peaks obtained for the hexagonal columnar phase acquires a shoulder in the lower temperature phase, which subsequently splits off into a separate peak as the temperature falls. This indicates that the hexagonal columnar structure of the hexagonal phase becomes distorted at lower temperatures finally resulting in the formation of rectangular columnar phase.

Table 1. The diffraction peaks intensities and inter-columnar distances [\AA] as a function of temperature [$^\circ\text{C}$] for dendritic LCP 1.

T [$^\circ\text{C}$]	No. of peaks	Intensity of first peak	Inter-columnar distance [\AA]
100	1 (110)	1.9	34.1
95	1	2.1	34.9
90	1	1.5	34.6
85	1	1.8	34.7
80	1	2.8	34.8
70	3 (110, 210, 220)	5.5	35.4
60	3	9.1	35.4
50	3	11.0	35.7
40	3	11.8	36.5
30	4	10.1	
20	4	10.4	

From the point of view of how the mesophases are formed, the presence of columnar mesophases suggests that the octasilsesquioxane dendrimer has a dislike gross molecular shape. The inter-columnar distance, however, is far too small for the long axes of the mesogens to be arranged in the planes of the dendritic discs, that is, like spokes in a wheel. An alternative model could be one in which the long axes of the mesogenic units are perpendicular or near perpendicular to the disc, see Figure 3. This proposed conformational organ-

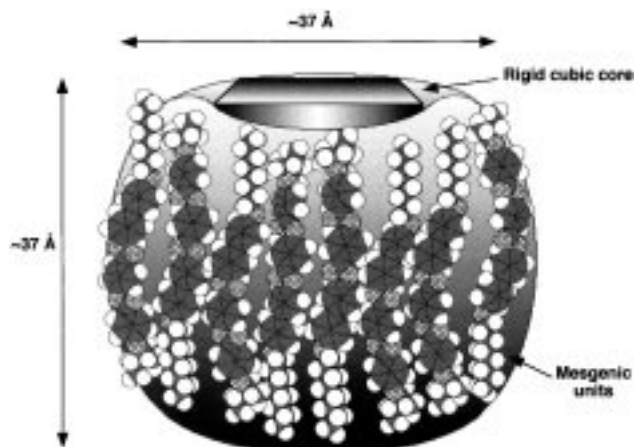


Figure 3. Schematic representation of the conformational structure of the dendritic disc.

ization of the dendrimer, and also a model of the structure of the disordered hexagonal columnar phase, are shown together in Figure 4. In this model, the octasilsesquioxane core units are stacked along the column axes with the mesogenic units arranged in a disordered way in-between the column axes.

Simple computer modeling (ChemDraw 3D) of segments of the dendrimer was used to investigate the structural organization of the system further. Simulations of the mesogenic moieties, without their lateral side chains, in the gas phase at absolute zero, gave the average length of the mesogenic units as approximately $37.5 \pm 1 \text{ \AA}$, which is the same as the inter-columnar distance. This could imply that the molecular discs are arranged in a fashion similar to that found for phasmidic liquid crystals. However, with sixteen mesogens involved in the assembly this seems highly unlikely.



Figure 4. A schematic representation of the structure of the disordered hexagonal columnar phase of dendritic LCP **1**. The octasilsesquioxane core is shown as the top of a ball with the mesogenic units forming a “cloud” about them.

Alternatively, if we now consider the cotton-reel model, simulations of the dendrimer minus the mesogenic arms gives a diameter for the dendritic disc of approximately 38–41 Å, which is close in value to the measured inter-columnar distance. Moreover, when sixteen mesogenic units (minus their lateral attachments) were assembled together to give a close-packed cylinder of mesogens, that is, irrespective of the presence of the octasilsesquioxane core, the diameter of the resulting cylinder was determined to be approximately 37–40 Å, see Figure 5. From these simulations, it appears that the

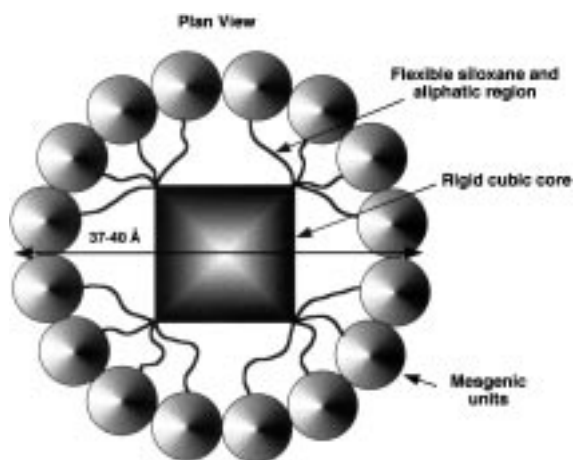


Figure 5. The cross-sectional area of the proposed dendritic disc with the mesogenic units just touching. The octasilsesquioxane cube lies approximately at the center, floating in a sea of flexible siloxane and aliphatic chains.

best fit to the data is obtained when, in the hexagonal phase, the dendrimer assumes a cylindrical shape that has approximately the same height as its diameter, as in Figure 3. The long axes of the mesogenic units are roughly parallel to or with a slight tilt with respect to the rotational axis that is normal to the cylinder, and that they are packed together side-by-side on the outer surface of the cylinder.

The situation is less clear with the chiral nematic phase. Two possibilities arise, one in which the dendritic molecules assume the cotton-reel structure and thus self-organize to give a chiral nematic discotic phase, see Figure 6, or alter-

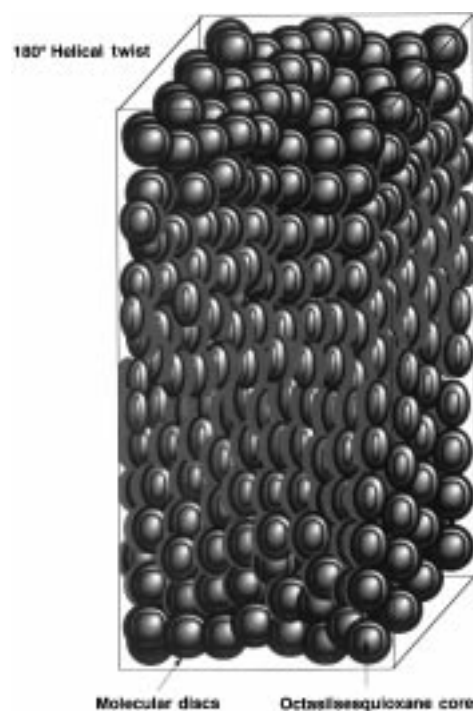


Figure 6. A proposed model for the chiral nematic discotic phase.

natively, the dendritic molecules might assume more of a rod-like shape, thereby self-organizing to give a chiral calamitic nematic phase, see Figure 7. It is difficult to envisage how this question might be resolved without detailed investigations of extremely well-aligned samples.

Thus the liquid crystalline behavior of dendrimer **1** emphasizes the role played by the octasilsesquioxane core when compared with related polysiloxanes.^[19c] A strict comparison of the transition temperatures is not possible since, although the degree of polymerization is above the “molecular weight effect”,^[20] the inner segments of the mesogenic structures are not identical. But even taking this into consideration, it is remarkable that the thermal stability of the N* phase is similar for the dendrimer with respect to related polysiloxanes, suggesting that the cubic core does not perturb significantly the associations between mesogens necessary to support the N* phase; whereas the observation of the formation of columnar phases for dendrimer **1**, but not for the corresponding polysiloxanes, indicates that the Si₈O₁₂ core assists in the interaction of neighboring mesogenic units resulting in the formation of such disordered structures.

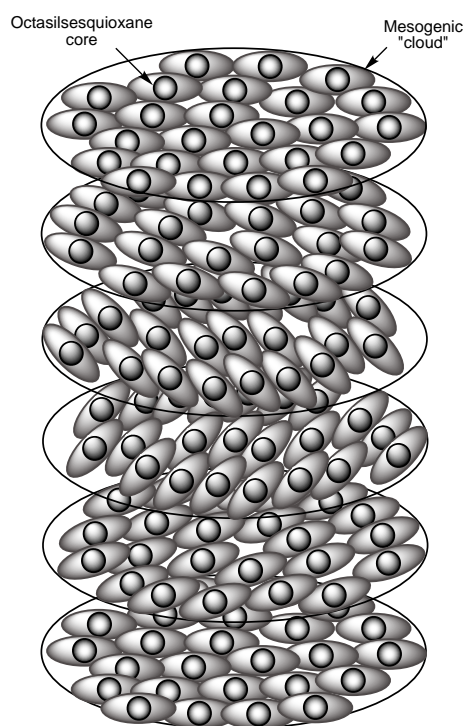


Figure 7. A proposed model for the chiral nematic calamitic phase.

Conclusion

Although there are aspects of this work that require further elucidation, the results presented in this study show that the N* phase is also represented among the mesophases displayed by the new dendritic liquid-crystal polymer architectures. The reported chiral nematic octasilsesquioxane dendrimer is relevant to the field of liquid-crystal displays based on light scattering,^[21] since the use of dendrimers in scattering electro-optical switches has also recently been reported.^[22]

Experimental Section

Solvents were rigorously dried over appropriate drying agents and distilled prior use. Low sulfur content, dry, degassed toluene and octavinyl octasilsesquioxane (Fluka), Karstedt's catalyst, and tetramethyldisiloxane (Fluorochem) were used as received. All atmosphere-sensitive reactions were carried out under dry nitrogen by using standard Schlenk techniques. Analytical TLC was performed on Kieselgel F-254 pre-coated silica gel plates (Merck). Visualization was accomplished with UV light or cerium and ammonium molybdate stain.

Infrared spectra were recorded on a Perkin–Elmer Paragon 1000 FT-IR spectrometer. NMR spectra were recorded on a Jeol JNM-LA (400 MHz) spectrometer; chemical shifts are reported in ppm (δ) with reference to internal SiMe₄ or residual protonated species of the deuteriated solvent used for ¹H analysis. Elemental analysis was performed on a Fisons Instruments Carlo Erba EA 1108 CHN analyzer with acetanilide as the reference standard. Mass spectra were recorded on a Finnigan 1020 GC-MS spectrometer (EI mode/70eV). Gel permeation chromatography was performed by using a set of 2 × 25 cm PL Gel Mixed-D columns (Polymer Laboratories), RI detector (Erma) 7510; the mobile phase was THF eluting at a flow rate of 1 mL min⁻¹, with toluene as flow marker. The molecular weight characteristics were established by using monodisperse polystyrene standards, with Polymer Laboratories Caliber software.

The mesomorphic properties of the materials were investigated by a combination of thermo-optical polarized light microscopy by using an

Olympus BH-2 polarized light microscope together with a Mettler FP52 microfurnace and FP5 temperature controller. The temperature controller was calibrated to an accuracy of $\pm 0.1^\circ\text{C}$ in the range 50–250°C. Phase transitions were determined by differential scanning calorimetry (DSC) by using a Perkin–Elmer DSC7-Series with Unix DSC data acquisition and analysis software at a scan rate of 10°C min⁻¹. The instrument was calibrated against pure indium metal (m.p. = 156.6°C, $\Delta H = 28.5\text{ J g}^{-1}$). Phase transition temperatures are reported as the endothermic onset temperature from differential scanning calorimetry traces. The diffraction measurements were made by using CuK α radiation from a sealed tube with other wavelengths removed by using a nickel filter and a graphite monochromator. The diffraction pattern was detected with a multi-wire area detector.^[23] It was placed at 840 mm from the sample with an evacuated path so that a Q (scattering vector) range from 0.03 Å⁻¹ to 0.5 Å⁻¹ was covered. The sample to detector distance was calibrated by using a silver behenate standard.^[24] Since the samples were not aligned, the scattering was regrouped so that pixels at the same radius were averaged, and the center of gravity of each diffraction peak was determined numerically and used to calculate its scattering vector. The precision of the Q values was generally better than 1%. The software for viewing and analysing the X-ray scattering was developed with PV-WAVE.^[25] The measurements were made at temperatures between 100°C and 20°C and, for instance at 70°C, peaks were found at $Q = 0.209, 0.357,$ and $0.407(4)\text{ Å}^{-1}$, which correspond to a hexagonal net with an inter-columnar distance of $35.4 \pm 0.4\text{ Å}$. Molecular simulations that were used as visual aids were created using ChemDrawPro 3D.

(S)-4'-Octyloxybiphenyl-4-yl 4-[4-(2-methylbutoxy)-2-(5-tetramethyldisiloxypentyl)oxy]benzoyloxy]benzoate (4): (S)-4'-Octyloxybiphenyl-4-yl 4-[4-(2-methylbutoxy)-2-(pent-4-enyloxy)benzoyloxy]benzoate (3)^[19c] (0.90 g, 1.30 mmol) in toluene (10 mL) was placed in a small Schlenk tube under nitrogen atmosphere. Karstedt's catalyst (3% Pt solution in xylene, 20 μL) was added and the solution stirred at room temperature 15 min; tetramethyldisiloxane (5.23 g, 39 mmol) was added, and the solution stirred 18 h at room temperature. The solvent and excess silane were evaporated under vacuum and the residue was purified by column chromatography (flash grade silica gel, *n*-hexane/diethyl ether 4:1, $R_f = 0.61$) to yield **4** as a milky syrup (0.630 g; 58%). K 73.6 ($\Delta H = 32.2\text{ kJ mol}^{-1}$) N* 88.2°C Iso ($\Delta H = 0.59\text{ kJ mol}^{-1}$); IR (KBr plates, thin film): $\bar{\nu} = 2120$ (s, Si–H), 1746, 1732 cm⁻¹ (s, C=O); ¹H NMR (400 MHz, CDCl₃, 24°C, internal CHCl₃): $\delta = 8.25$ (m, 2H; aromatic), 8.02 (m, 1H; aromatic), 7.58 (m, 2H; aromatic), 7.49 (m, 2H; aromatic), 7.35 (m, 2H; aromatic), 7.24 (m, 2H; aromatic), 6.96 (m, 2H; aromatic), 6.52 (m, 2H; aromatic), 4.64 (septet, $J = 2.5\text{ Hz}$, 1H; Si–H), 4.03 (t, $J = 6\text{ Hz}$, 2H; CH₂–O–Ph), 3.96 (t, $J = 6\text{ Hz}$, 2H; CH₂–O–Ph), 3.85 (m, 2H; O–CH₂–CH), 1.82 (m, 5H; CH₂–CH₂–O, CH, CH₂–CH₂–Si), 1.51 (m, 4H; (CH₂)_n), 1.31 (m, 12H; (CH₂)_n), 1.02 (d, $J = 6\text{ Hz}$, 3H; CH₃–CH), 0.95 (t, $J = 7\text{ Hz}$, 3H; CH₃–CH₂), 0.87 (t, $J = 6\text{ Hz}$, 3H; CH₃–CH₂), 0.50 (m, 2H; CH₂–SiOSiH), 0.12 (d, $J = 2.5\text{ Hz}$, 6H; (CH₃)₂Si–H), 0.02 (s, 6H; (CH₃)₂Si–CH₂); ²⁹Si NMR (79.3 MHz, CDCl₃, 24°C, external TMS): $\delta = 9.79$ (s, CH₂–SiOSi–H), -6.73 (s, CH₂–SiOSi–H).

Synthesis of 1: G₁-Vinyl₁₆ octasilsesquioxane dendrimer **2** (0.025 g, 0.017 mmol) was placed in a Schlenk tube and dissolved in dry, degassed toluene (4 mL) under nitrogen. Karstedt's catalyst (10 μL) added and the solution was aerated (30 s). The solution was stirred for 15 min. A solution of **4** (0.302 g, 0.366 mmol) in toluene (4 mL) was added, and the mixture stirred for 18 h. The solvent was removed under vacuum, and the residue dissolved in CH₂Cl₂ (2 mL) and precipitated by addition to methanol (150 mL) ($\times 3$). The precipitate was purified by column chromatography (flash grade silica gel, elution with CH₂Cl₂/0.6% diethyl ether; $R_f = 0.17$). The product was recovered and dried under vacuum. Yield: 0.090 g (35%) white tacky material; elemental analysis calcd (%) for C₈₂₄H₁₁₆₀O₁₄₀Si₄₈: C 67.54, H 7.97; found C 66.86, H 8.34; ¹H NMR (400 MHz, CDCl₃, 24°C, internal CHCl₃): $\delta = 8.20$ (m, 4H; aromatic), 8.01 (m, 2H; aromatic), 7.53 (m, 4H; aromatic), 7.45 (m, 4H; aromatic), 7.29 (m, 4H; aromatic), 7.20 (m, 4H; aromatic), 6.93 (m, 4H; aromatic), 6.47 (m, 4H; aromatic), 3.95 (m, 8H; CH₂–O–Ph), 3.78 (d $J = 16\text{ Hz}$, 4H; O–CH₂–CH), 1.80 (m, 10H; CH₂–CH₂–O, CH, CH₂–CH₂–Si), 1.51 (m, 8H; (CH₂)_n), 1.28 (m, 24H; (CH₂)_n), 0.49 (m, 8H; CH₂–SiOSi–CH₂), 0.34 (m, 8H; ≡Si–CH₂–, CH₂–Si–CH₂), 0.00 (2s, 24H; CH₃–Si–O), -0.10 (s, 3H; CH₃Si(CH₂–CH₂)₃); ²⁹Si NMR (79.3 MHz, CD₂Cl₂, 24°C, external TMS): $\delta = 8.30, 7.93$ (s, CH₂–SiOSi–CH₂), 7.23 (s, CH₃–Si(CH₂–CH₂)₃), -66.36 (Si₈O₁₂).

Acknowledgements

The authors are very grateful to The Leverhulme Trust for financial support for a Research Fellowship. Dr. H. Snelling and C. Walton, Department of Physics, University of Hull, are acknowledged for MALDI spectrometry measurements.

- [1] G. R. Newkome, C. N. Moorefield, F. Vögtle, *Dendritic Molecules: Concepts, Syntheses, Perspectives*, VCH, Weinheim **1996**; latest reviews: a) "Dendrimers": *Top. Curr. Chem.* **1998**, *197*, whole issue; b) A. Archut, F. Vögtle, *Chem. Soc. Rev.* **1998**, *27*, 233; c) H. Frey, C. Lach, K. Lorenz, *Adv. Mater.* **1998**, *10*, 279; d) V. V. Tsukruk, *Adv. Mater.* **1998**, *10*, 253; e) F. Zheng, S. C. Zimmerman, *Chem. Rev.* **1997**, *97*, 1681; f) M. Fischer, F. Vögtle, *Angew. Chem.* **1999**, *111*, 934; *Angew. Chem. Int. Ed.* **1999**, *38*, 884; g) A. W. Bosman, H. M. Janssen, E. W. Meijer, *Chem. Rev.* **1999**, *99*, 1665; h) D. K. Smith, F. Diederich, *Chem. Eur. J.* **1998**, *4*, 1353; i) C. W. Thomas, Y. Tor, *Chirality*, **1998**, *53*, and references therein.
- [2] a) V. Percec, M. Kawasumi, *Macromolecules*, **1992**, *25*, 3843; b) V. Percec, P. Chu, G. Ungar, J. Zhou, *J. Am. Chem. Soc.* **1995**, *117*, 11 441.
- [3] S. Bauer, H. Fischer, H. Ringsdorf, *Angew. Chem.* **1993**, *105*, 1658; *Angew. Chem. Int. Ed. Engl.* **1993**, *32*, 1589.
- [4] a) U. Stebani, G. Lattermann, M. Wittenberg, J. Wendorff, *Angew. Chem.* **1996**, *35*, 1858; *Angew. Chem. Int. Ed. Engl.* **1996**, *35*, 1585; b) J. H. Cameron, A. Facher, G. Lattermann, S. Diele, *Adv. Mater.* **1997**, *9*, 398.
- [5] a) V. Percec, W. D. Cho, P. E. Mosier, G. Ungar, D. J. P. Yearly, *J. Am. Chem. Soc.* **1998**, *120*, 11 061; b) V. Percec, C.-H. Ahn, T. K. Bera, G. Ungar, D. J. P. Yearly, *Chem. Eur. J.* **1999**, *5*, 1070; c) G. Ungar, V. Percec, M. Holerca, G. Johansson, J. A. Heck, *Chem. Eur. J.* **2000**, *6*, 1258; d) V. Percec, W.-D. Cho, G. Ungar, D. J. Yearley, *Angew. Chem.* **2000**, *112*, 1661; *Angew. Chem. Int. Ed.* **2000**, *39*, 1598, and references therein.
- [6] D. J. Pesak, J. S. Moore, *Angew. Chem.* **1997**, *109*, 1709; *Angew. Chem. Int. Ed. Engl.* **1997**, *36*, 1636.
- [7] a) H. Meier, M. Lehmann, *Angew. Chem.* **1998**, *110*, 666; *Angew. Chem. Int. Ed. Engl.* **1998**, *37*, 643; b) H. Meier, M. Lehmann, U. Kolb, *Chem. Eur. J.* **2000**, *6*, 2462.
- [8] a) K. Lorenz, D. Hölter, B. Stühn, R. Mülhaupt, H. Frey, *Adv. Mater.* **1996**, *8*, 414; b) K. Lorenz, H. Frey, B. Stühn, R. Mülhaupt, *Macromolecules*, **1997**, *30*, 6860.
- [9] a) S. A. Ponomarenko, E. A. Rebrov, A. Y. Bobrovsky, N. I. Boiko, A. M. Muzafarov, V. P. Shibaev, *Liq. Cryst.* **1996**, *21*, 1; b) S. A. Ponomarenko, E. A. Rebrov, N. I. Boiko, A. M. Muzafarov, V. Shibaev, *J. Polym. Sci. Part A* **1998**, *40*, 763; c) R. M. Richardson, S. A. Ponomarenko, N. I. Boiko, V. P. Shibaev, *Liq. Cryst.* **1999**, *26*, 101; d) S. A. Ponomarenko, N. I. Boiko, V. P. Shibaev, R. M. Richardson, I. J. Whitehouse, E. A. Rebrov, A. M. Muzafarov, *Macromolecules*, **2000**, *33*, 5549.
- [10] D. Terunuma, R. Kato, R. Nishio, K. Matsuoka, H. Kuzuhara, Y. Aoi, H. Nohira, *Chem. Lett.* **1998**, 59.
- [11] a) R. Deschenaux, E. Serrano, A.-M. Levelut, *Chem. Commun.* **1997**, 1577; b) B. Dardel, R. Deschenaux, M. Even, E. Serrano, *Macromolecules*, **1999**, *32*, 5193.
- [12] P. Busson, H. Ihre, A. Hult, *J. Am. Chem. Soc.* **1998**, *120*, 9070.
- [13] a) K. Suzuki, O. Haba, R. Nagahata, K. Yonetake, M. Ueda, *High Perform. Polym.* **1998**, *10*, 231; b) J. Barberá, M. Marcos, A. Omenat, J. L. Serrano, J. I. Martínez, P. J. Alonso, *Liq. Cryst.* **2000**, *27*, 255.
- [14] a) M. W. P. L. Baars, S. H. M. Söntjens, H. M. Fischer, H. W. I. Peerlings, E. W. Meijer, *Chem. Eur. J.* **1998**, *4*, 2456; b) J. Barberá, M. Marcos, J. L. Serrano, *Chem. Eur. J.* **1999**, *5*, 1834; c) K. Yonekate, K. Suzuki, T. Morishita, R. Nagahata, M. Ueda, *High Perform. Polym.* **1998**, *10*, 373; d) K. Yonetake, T. Masuko, T. Morishita, K. Suzuki, M. Ueda, R. Nagahata, *Macromolecules* **1999**, *32*, 6578.
- [15] I. M. Saez, J. W. Goodby, *Liq. Cryst.* **1999**, *26*, 1101.
- [16] a) F.-H. Kreuzer, R. Maurer, P. Spes, *Makromol. Chem. Macromol. Symp.* **1991**, *30*, 215; b) A. Sellinger, R. M. Laine, V. Chu, C. Viney, *J. Polym. Sci. Part A* **1994**, *32*, 3069; c) G. H. Mehl, J. W. Goodby, *Angew. Chem.* **1996**, *105*, 2791; *Angew. Chem. Int. Ed. Engl.* **1996**, *35*, 2641; d) I. M. Saez, P. Styring, *Adv. Mater.* **1996**, *8*, 1001; e) J. W. Goodby, G. H. Mehl, I. M. Saez, R. P. Tuffin, G. Mackenzie, R. Auzely-Velty, T. Benvegnu, D. Plusquellec, *Chem. Commun.* **1998**, 2057; f) R. M. Laine, C. Zhang, A. Sellinger, L. Viculis, *Appl. Organomet. Chem.* **1998**, *12*, 715; g) G. H. Mehl, I. M. Saez, *Appl. Organomet. Chem.* **1998**, *13*, 261; h) G. H. Mehl, A. J. Thornton, G. W. Goodby, *Mol. Cryst. Liq. Cryst. Sci. Technol. Sect. A* **1999**, *332*, 2965; i) R. Elsäßer, G. H. Mehl, J. W. Goodby, D. J. Photinos, *Chem. Commun.* **2000**, 851.
- [17] P.-A. Jaffrès, R. E. Morris, *J. Chem. Soc. Dalton Trans.* **1998**, 2767.
- [18] *Handbook of Liquid Crystals, Vol. 2A*, (Eds.: D. Demus, J. W. Goodby, G. W. Gray, H. W. Spiess, V. Vill), Wiley-VCH, Weinheim, **1998**.
- [19] a) F. Hessel, H. Finkelmann, *Polym. Bull.* **1985**, *14*, 375; b) G. W. Gray, J. S. Hill, D. Lacey, *Angew. Chem.* **1989**, *101*, 1146; *Angew. Chem. Int. Ed. Engl.* **1989**, *28*, 1120 (*Adv. Mater.* **1989**, *1*, 292); c) R. Lewthwaite, J. W. Goodby, K. J. Toyne, *J. Mater. Chem.* **1993**, *3*, 241.
- [20] V. Percec, P. Tomazos, C. Pugh, *Macromolecules*, **1989**, *22*, 3259.
- [21] *Liquid Crystals in Complex Geometries Formed by Polymers and Porous Networks* (Eds.: G. P. Crawford, S. Zumer), Taylor and Francis, London, **1996**.
- [22] a) M. W. P. L. Baars, M. C. W. van Boxtel, C. W. M. Bastiaansen, D. J. Broer, S. H. M. Sönjens, E. W. Meijer, *Adv. Mater.* **2000**, *12*, 715; b) M. C. W. van Boxtel, D. J. Broer, C. W. M. Bastiaansen, M. Baars, R. Janssen, *Macromol. Symposia* **2000**, *154*, 25.
- [23] J. E. Bateman, J. F. Connolly, R. Stephenson, A. C. Flesher, C. J. Bryant, A. D. Lincoln, P. A. Tucker, S. W. Swanton, *Nucl. Instrum. Methods Phys. Res. Sect. A* **1987**, *259*, 506.
- [24] T. C. Huang, H. Toraya, T. N. Blanton, Y. Wu, *J. Appl. Cryst.* **1993**, *26*, 180.
- [25] supplied by Visual Numerics. <http://www.vni.com/products/wave/index.html>.

Received: November 27, 2000 [F2903]